

# Fast and Robust Experimental Evaluation Methods for Microfluidic Mixers

*Jonas Kluitmann<sup>1</sup>, Xie Xie<sup>1</sup>, Oliver Blaschke<sup>1</sup>, Jakob Elsner<sup>1</sup>, Klaus Stefan Drese<sup>1</sup>*

<sup>1</sup> ISAT – Institute of Sensor and Actuator Technology

Coburg University of Applied Sciences and Arts; Am Hofbräuhaus 1b; 96450 Coburg, Germany

*jonas.kluitmann@hs-coburg.de*

## Summary:

For the evaluation, classification and the later basis for process and equipment design of microfluidic mixers, we present a comparison of two experimental methods, their mode of analysis and a comparison of the analytic results. We acquire the mixing states at multiple locations along a mixer and thereby reduce the error due to local fluctuations. Data was acquired for a range of Reynolds numbers between 0.5 and 400 for the two different model mixing processes. The different model mixing processes require different data processing. Despite the difference in the acquired data and the analyses, we show in a comparison that the evaluation methods lead to comparable results. The comparability is albeit limited by an upper Reynolds number boundary at which the results diverge.

**Keywords:** Microfluidics, Passive Mixing, Dean Mixer, Mix Norm, Mixer Characterization

## Background, Motivation an Objective

The mixing of reactant streams is an important part of many processes in chemistry, biotechnology and analytics. Bad mixing can result in bad product outcomes or unreliable analyses. In microfluidic applications, mixing is not a trivial task since the influence of viscous forces dominates over inertial forces at shrinking dimensions. The ratio of these forces is characterized by the Reynolds number,  $Re$ .

At small dimensions, laminar flow is usually predominant and fluid streams do not interfuse. Mass transport between the stratified streamlines occurs mainly diffusive. The induction of turbulent flows that would facilitate mixing is challenging. Hence, many operation principles for mixers have been developed to facilitate mixing and countless designs have been implemented.

Despite these efforts no “perfect” mixer has been found so far. A mixer must be adapted to the requirements of the target process. Important target criteria include the mixing time, integration space, shear sensitivity, dead volume, mass throughput or pressure loss. Further constraints may be added by production technology and material choice, target mixing quality or energy efficiency.

To evaluate a mixer for its application suitability, a characterization is usually necessary to confirm planned and simulated properties. To characterize mixers, several methods are being

used. Popular methods often use changes in the colors of the streams being mixed. These color changes allow for a facile, optical evaluation of the mixing process. We will focus on the dilution of a dye and the reaction of iron(III) with thiocyanate ions as a color reaction that can be regarded as instantaneous for the purposes of this mixer characterization [1].

While the dye dilution is a popular and easy to model for mixing systems, it has several drawbacks. The concentration of the dye averaged over the channel cross section is constant over all locations of a mixer. As a consequence of this, the intensity of the dye in a projection over the channel’s cross section remains constant over the mixer length. Hence, the dye and thus color distribution, is used to quantify the mixing process with different models. A rotation of parts of the fluid streams can however cause misleading outcomes, since the information on the distribution of the fluid streams is contained in the cross section of the channel while the projection of the cross section is usually obtained. By obtaining images of fluorescence intensity distributions in channel cross sections [2], or obtaining images in different projection directions [3], this problem can be mitigated at the expense of higher cost and complexity.

The use of color reactions can circumvent this problem. Since the absorbing species is formed in the process upon contact of the reactants, there is a progressively stronger coloration with the progressing mixing process. This type of

model reaction however necessitates a different data analysis. When using measures for the distribution of intensities as for the dye dilution, the assignment of mixing states to the measurement number is not expected to be bijective. For the use of two non-colored educts, a homogenous, colorless intensity distribution at the beginning evolves into an inhomogeneous distribution in the incomplete mixing process and turns into a colored, homogenous distribution when the mixing process is completed. Instead of measures for the intensity distribution, the absolute color intensity can directly be taken as a measure for the progress of the mixing process.

### Description of the New Method or System

Microfluidic reactors were produced in-house. A fluidic design was sliced horizontally into layers. Vector files for the single layers were created using Inkscape. The layers were cut into Polycarbonate films of 125  $\mu\text{m}$  thickness using a CO<sub>2</sub>-Lasercutter. After cleaning the structured layers in isopropyl alcohol and water, the layers were stacked in order and dried in a vacuum oven at 130 °C for three hours. After drying, the stacks were realigned and clamped between two microscopy slides. At 190 °C, the clamped assemblies were incubated at ambient pressure for 3 minutes, after which a vacuum was applied for 3.5 minutes.

For this study, Dean mixers were used, as shown in Fig. 1b.

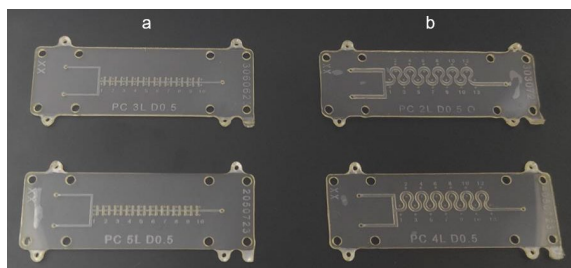


Fig. 1. Photographs of the microfluidic mixers, H-type mixer (a) and Dean mixer (b). The mixer dimensions are 75x25 mm.

Dye dilution experiments were conducted using a 4:100 diluted ink (Pelikan 4001 dark-green) and water as diluent. The color reaction was conducted by mixing 20 mM Fe(NO<sub>3</sub>)<sub>3</sub> and 60 mM NaSCN, both dissolved in 99.5 % ethanol. The flow rates to reach determined  $Re$  were set using syringe pumps.

Images of the mixing process were acquired in a bright field microscope with a mounted camera at a fixed illumination and exposure. The mixer chips contained markers in equidistant positions for aligning the chips and reproducibly analyzing positions.

The acquired images were cropped to the channel area using a Python script recognizing aligning markers and the channel boundaries by their contrast. The RGB images were converted into grayscale with different weightings of the channels based on the absorbance spectra of the detected species.

For all experiments, a mix norm and normalized intensity mean derived value was calculated from the extracted grayscale lines.

The mix norm used is as proposed by Mathew et al. [4]:

$$\Phi = \sqrt{\sum_k \frac{|a_k|}{\sqrt{1 + 4\pi^2 k^2}}} \quad (1)$$

With the mix norm  $\Phi$ , the wavenumber  $k$ , and the correlated Fourier coefficients  $a_k$ .

For the mean derived value, the intensity over the channel position for the experiment condition was calculated and corrected against the mean intensity of that channel position with only solvent filled into the channel. The data was normalized by subtracting the mean intensity of the channel position when filled with preformed iron thiocyanate or ink solution, respectively, and dividing by the difference of the mean intensities of the solvent-filled channel and the intensity of the channel filled with the respective colored solution.

### Results

The images of the channel contents along the mixer are shown in Fig. 2 and Fig. 5 for the model reaction of iron and thiocyanate ions and the dilution of ink, respectively.

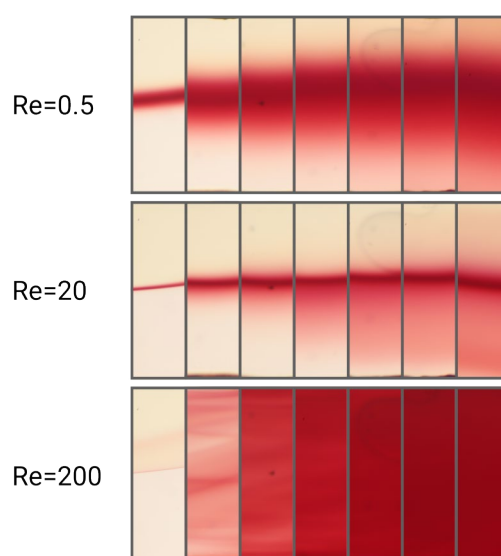


Fig. 2. Images of the channel contents for a color reaction yielding Fe(SCN)<sub>3</sub> along a microfluidic Dean mixer at Reynolds numbers of 0.5; 20 and 200. Images in the same column were taken at the same position in the same chip.

For the reaction of iron(III) with thiocyanate ions, there are colorless areas at the channel walls at the mixer entry with an intensely red colored line at the center of the channel, where the colored compound is formed. With a rising  $Re$ , the width of the colored line shrinks at the inlet and the coloration intensity falls. Since  $Re$  is proportional to the flow rate, this can be explained with a longer residence time of the fluid packets in the channel at the location of imaging, leading to a longer interdiffusion time and more product formation.

For  $Re=0.5$  there is a progressive widening of the colored area towards both channel walls with a falling color intensity from the center towards the channel walls. At  $Re=20$ , the observations remain identical. However, the width of the central colored line is narrower compared to the process at  $Re=0.5$  and shows an asymmetric radial distribution of the coloration to the channel walls.

At  $Re=200$ , there are multiple lines of colored reaction products visible across the channel. With a progressing location along the chip, the overall coloration intensity rises, until at the sixth and seventh position, the channel area is homogeneously red. The formation of the multiple lines is attributed to the formation of vortices in the Dean mixer at elevated flow rates and hence Dean number and  $Re$ . These vortices support the mixing in the curved channels. [5]

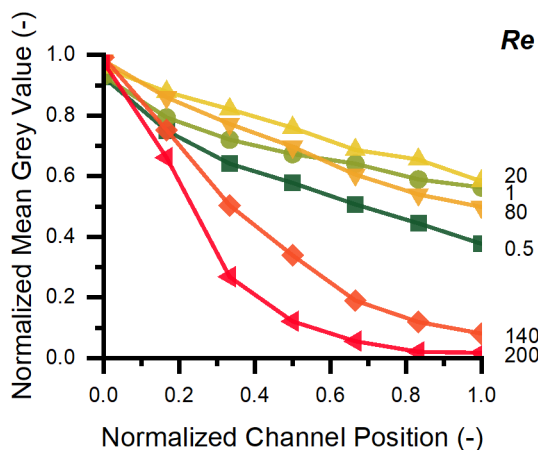


Fig. 3. Plot of the normalized mean grey value over the normalized channel position for a color reaction yielding  $Fe(SCN)_3$  in a microfluidic Dean mixer at different Reynolds numbers.

The normalized intensity values for the channel contents of the mixing process along the channel are shown in Fig. 3. The normalized mean grey values start at a value of close to one and fall towards zero. Starting from  $Re=0.5$ , the grey value falls slower with an increasing  $Re$  until  $Re=20$ , at which point the decline of the grey

value over the channel positions accelerates with rising  $Re$ .

This result must not be mistaken for a temporally slower mixing at  $Re=20$  compared to  $Re=0.5$ . In Fig. 3 and Fig. 7 the data is plotted over the normalized channel position. A normalized mixing time can be obtained by dividing the normalized channel position by the flow velocity, which is proportional to  $Re$ .

The diverging values at the channel position zero are attributed to the reaction beginning at the moment of fluid contact, the reaction product immediately appears and the coloration is stronger for longer contact times, i.e. lower  $Re$ .

The observations for the ink dilution as shown in Fig. 5 are analogous to the observations for the color reaction. Instead of the formation of color, the sharpness of the color separation in the channel center can be observed for this case.



Fig. 5. Images of the channel contents for an ink dilution along a microfluidic Dean mixer at Reynolds numbers of 0.5. The channel positions match those in Fig. 2.

The median grey value of the channels are constant over all channel positions for one flow condition with small variations between the different flow conditions, with higher flow rates connected to lower grey values. (Data not shown)

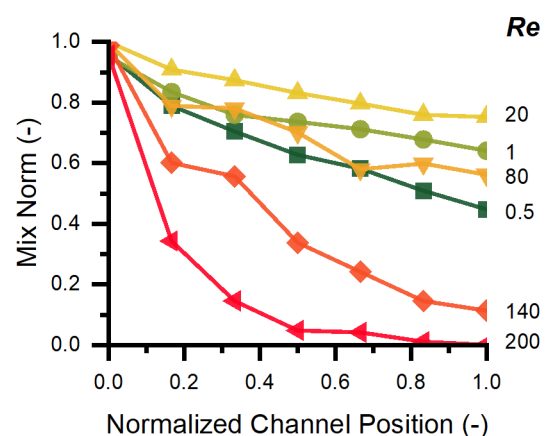


Fig. 6. Plot of the mix norm over the normalized channel position for an ink dilution in a microfluidic Dean mixer at different  $Re$ .

When the mix norm for the ink dilution is plotted over the channel positions as in Fig. 6, the

trends and values for the mix norm for each  $Re$  as well as the relation of the positions of the trends of different  $Re$  to one another show a very close relation to those of the normalized mean grey values of the iron(III) thiocyanate reaction in Fig. 3.

The presence of multiple sampling points for one flow condition allows for a more robust performance evaluation and allows for a correction of outliers. For this purpose, the trends of the characterizing quantities as shown in Fig. 3 and Fig. 6 were fit onto an exponential decay model:

$$f(x) = Ae^{-Bx} + C \quad (2)$$

The fit parameter  $B$  determining the decay velocity of the observed value is then plotted over  $Re$  for both model systems as shown in Fig. 7. Fits with an  $R^2$ -Value of 0.9 and below were rejected.

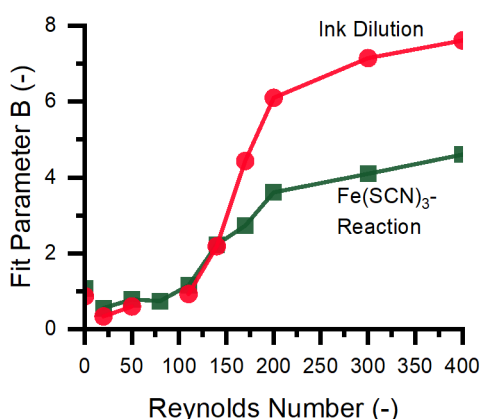


Fig. 7. Plot of the mixing velocity indicating fit parameter  $B$  over  $Re$  position for both model reactions and analyses.

The characterization of the mixing process through one quantity for one flow condition allows comparison of the mixing evaluation data of the two models.

For low  $Re \leq 140$  the plot shows a good agreement of the parameter  $B$  between both evaluation methods. At higher  $Re$ , there is however a deviation between both trends. For the ink dilution, parameter  $B$  rises strongly until  $Re=200$ , while the increase for that parameter in the thiocyanate reaction is slower. At values of  $Re > 200$ , the increase in  $B$  slows down considerably. This divergence at higher  $Re$  is not expected, as the mixing velocity and hence  $B$  were expected to match between both models.

The reason for the divergence is unexplained. A different effect of the different analysis methods upon the formation of flow structures as in

Fig. 2 for  $Re=200$ , panel 2 is possible. The structures indicating secondary flows however already emerge at  $Re=50$ , well below the start of the divergence.

It is possible that at high concentrations of the colored complex, the images are acquired outside of the linear range of the camera sensor. This can occur if one or more sub-pixels reach a value close to zero due to a high absorbance. In this case almost all light for these sub-pixels is absorbed by the sample, so that an increase in concentration of the colored species does not affect these sub-pixels anymore. Sub-pixels that register light at a wavelength band that is absorbed weaker, for the iron(III) thiocyanate, this is the red sub-pixel, the measured absorbance still rises with the concentration, albeit slower than for the dark subpixels in their linear range. When the dark sub-pixels are included in the conversion into the greyscale image, this effect will lead to an apparent slow-down in the mixing, once one sub-pixel turns dark. This problem could be mitigated by lowering the concentration of the reactants or raising the illumination strength.

Since the difference in the trend of the parameter  $B$  between the different methods and data processing steps is not solved, further evaluation of the comparability of these two methods is needed.

### Acknowledgements

This work has been done within the BioQuant project, funded by the German Federal Ministry for Education and Research, BMBF (031B1124B).

### References

- [1] K. C. De Berg, *The Iron(III) Thiocyanate Reaction: Research History and Role in Chemical Analysis*. in SpringerBriefs in Molecular Science. Cham: Springer International Publishing, 2019. doi: 10.1007/978-3-030-27316-3.
- [2] A. D. Stroock, S. K. W. Dertinger, A. Ajdari, I. Mezić, H. A. Stone, and G. M. Whitesides, "Chaotic Mixer for Microchannels," *Science*, vol. 295, no. 5555, pp. 647–651, Jan. 2002, doi: 10.1126/science.1066238.
- [3] V. S. Duryodhan, R. Chatterjee, S. Govind Singh, and A. Agrawal, "Mixing in planar spiral microchannel," *Experimental Thermal and Fluid Science*, vol. 89, pp. 119–127, Dec. 2017, doi: 10.1016/j.expthermflusci.2017.07.024.
- [4] G. Mathew, I. Mezić, and L. Petzold, "A multiscale measure for mixing," *Physica D: Nonlinear Phenomena*, vol. 211, no. 1–2, pp. 23–46, Nov. 2005, doi: 10.1016/j.physd.2005.07.017.
- [5] F. Jiang, K. S. Drese, S. Hardt, M. Küpper, and F. Schönfeld, "Helical flows and chaotic mixing in curved micro channels," *AIChE Journal*, vol. 50, no. 9, pp. 2297–2305, Sep. 2004, doi: 10.1002/aic.10188.